Tautomer Selection Through Solvate Formation: The Case of 5-Hydroxynicotinic Acid

Abhinav Joseph,[a,†] Joana S. Rodrigues Alves,[a] Carlos E. S. Bernardes,[a,b] M. Fátima M. Piedade,[a,b] and Manuel E. Minas da Piedade*,[a]

[a] *Centro de Química e Bioquímica and Centro de Química Estrutural, Faculdade de Ciências, Universidade de Lisboa, 1749-016 Lisboa, Portugal; E-mail: memp@fc.ul.pt*

[b] *Centro de Química Estrutural, Complexo Interdisciplinar, Instituto Superior Técnico da Universidade Técnica de Lisboa, 1049-001 Lisboa, Portugal.*

KEYWORDS: tautomerism / 5-hydroxynicotinic acid / crystal engineering / hydrate / solvate / crystal structure / X-ray diffraction / DRIFT / thermodynamics / calorimetry / thermal analysis

† Current address: Division of Research and Development, Lovely Professional University, Phagwara, Punjab, 144411, India.

Supporting Information

Table S1. Indexation of the X-Ray Powder Diffraction Pattern of 5HNA·H_2O Recorded at 295±2 K, in the Range 5º≤ 2θ ≤ 35º; Space Group $P2_1/c$; a = 4.491(3) Å, b = 16.414(6) Å, c = 9.034(4) Å, β = 89.98(1).

h	k	l	2θ(obs)/º	$\Delta 2\theta$/º
0	2	0	10.80	0.02
0	1	1	11.19	0.01
0	2	1	14.58	0.00
0	3	1	18.95	-0.01
0	0	2	19.65	0.00
0	1	2	20.39	0.00
0	4	0	21.67	0.02
0	2	2	22.46	-0.01
0	4	1	23.81	-0.01
1	2	1	24.60	-0.05
0	3	2	25.57	0.00
1	0	2	28.02	0.01
1	1	2	28.57	0.03
0	4	2	29.41	0.00
1	2	2	30.11	0.02
0	6	0	32.74	0.01
0	5	2	33.75	-0.01

Table S2. Indexation of the X-Ray Powder Diffraction Pattern of 5HNA·DMSO Recorded at 295±2 K, in the Range 5º≤ 2θ ≤ 35º; Space Group $P2_1/c$; a = 5.283(5) Å, b = 22.671(14) Å, c = 8.558(6) Å, β = 93.23(13).

h	k	l	2θ(obs)/º	$\Delta 2\theta$/º
0	2	0	7.79	0.00
0	2	1	12.94	-0.03
0	4	0	15.66	0.04
0	4	1	18.79	0.01
-1	1	1	19.65	-0.01
1	1	1	20.64	0.00
-1	2	1	20.83	0.02
0	1	2	21.13	-0.02
1	2	1	21.72	-0.02
0	2	2	22.22	0.00
-1	3	1	22.62	0.02
1	4	0	23.01	-0.01
0	6	0	23.54	0.01
0	3	2	23.91	0.00
-1	4	1	24.90	0.00
0	6	1	25.79	0.03
-1	0	2	26.00	-0.07
0	4	2	26.09	-0.01
-1	1	2	26.38	0.01
-1	2	2	27.30	0.05
1	1	2	27.88	0.01
1	2	2	28.72	0.02
1	3	2	30.05	0.00
-1	6	1	30.53	-0.05
0	6	2	31.54	-0.05
0	2	3	32.42	0.03
-1	5	2	32.83	0.03

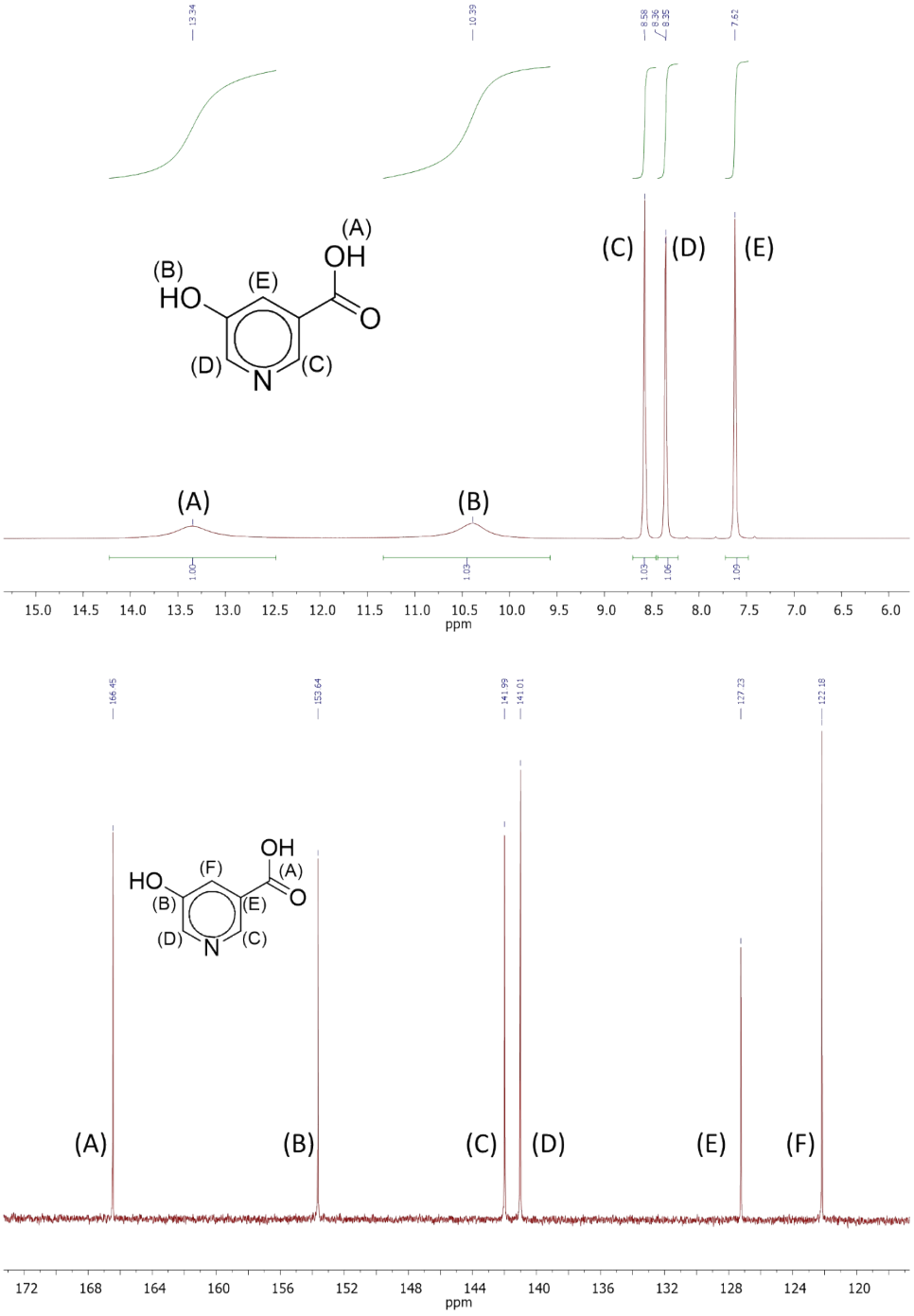

Figure S1. ^{1}H-NMR (top) and ^{13}C-NMR (bottom) spectra of 5-hydroxynicotinic acid recorded at ambient temperature in DMSO-d_6. Chemical shifts are given relative to TMS.

Time evolution of 5HNA·H_2O and 5HNA·DMSO samples thermally treated for 30 min at 360 K. Samples of 5HNA·H_2O and 5HNA·DMSO were kept at 360 K for 30 min, cooled to 295±2 K, and monitored at that temperature, by powder X-ray diffraction for one year. The obtained powder patterns are compared in Figure S2 with that of the unsolvated 5HNA starting material obtained by sublimation.

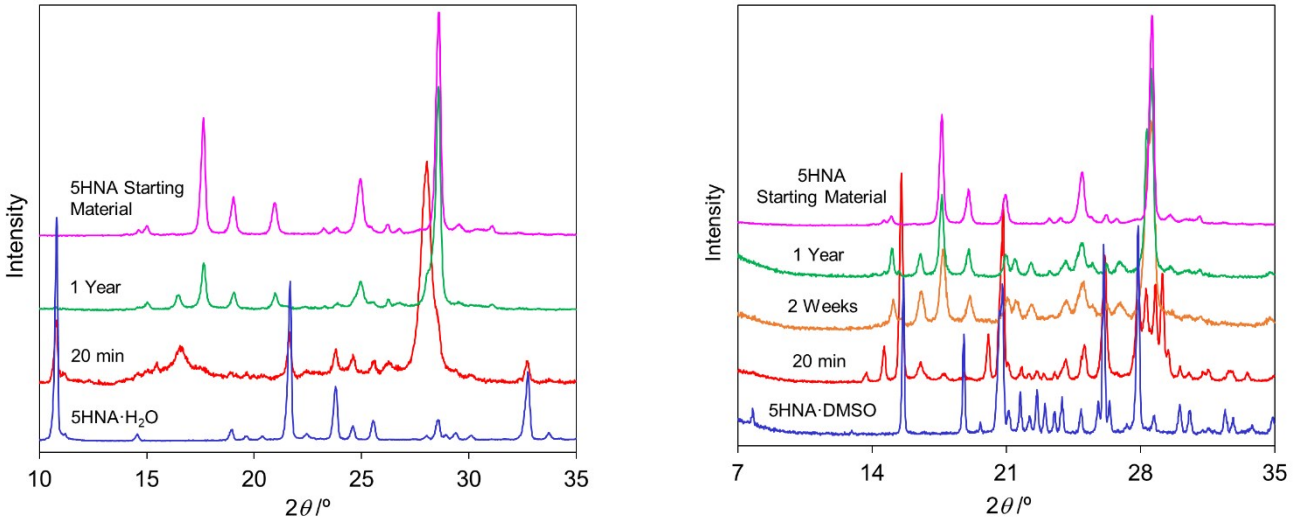

Figure S2. Time evolution of the powder X-ray diffraction patterns of (a) 5HNA·H_2O and (b) 5HNA·DMSO samples thermally treated for 30 min at 360 K and cooled to 295±2 K. Also shown is the pattern of the 5HNA starting material obtained by sublimation.

Slurry test on 5HNA·H_2O. A suspension of 5HNA·H_2O in water was kept under magnetic stirring for two days at 293.0±0.1 K. The powder pattern of the obtained material is compared in Figure S3 with those of the original 5HNA·H_2O sample and the sublimed 5HNA anhydrate.

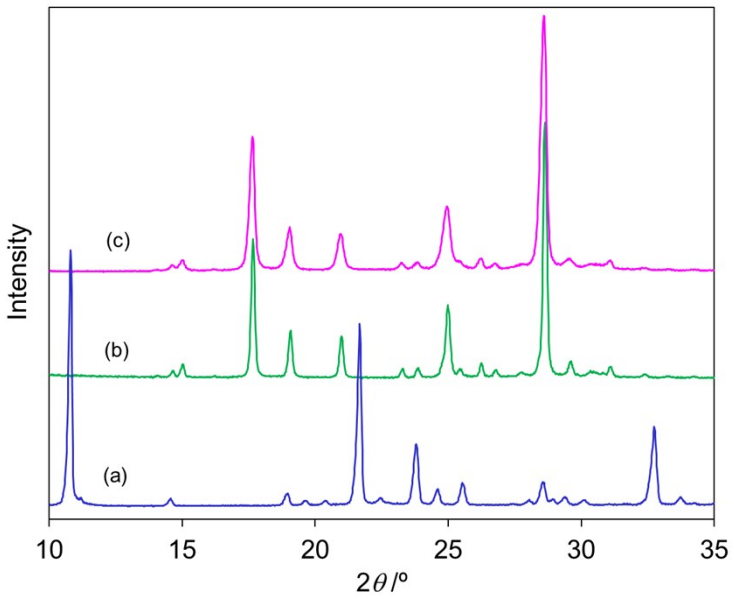

Figure S3. Results of the slurry test on 5HNA·H_2O carried out in water at 293.0±0.1 K during two days. Powder X-ray diffraction patterns of: (a) the initial 5HNA·H_2O sample; (b) the material obtained after two days equilibration in water; (c) the 5HNA starting material obtained by sublimation.

Thermogravimetry (TG). The results of the determination of the molar fraction n of water and DMSO in 5HNA·nH$_2$O and 5HNA·nDMSO by TG at a heating rate $\beta = 5$ K·min^{-1} are summarized in Tables S3 and S4. Here, T_i and T_f are the initial and final temperatures of the mass loss step, m_i is the initial mass of sample, and Δm is the observed mass loss. The uncertainties quoted for $\langle T_i \rangle$, $\langle T_f \rangle$ and $\langle n \rangle$, represent twice the standard error of the mean. Figure S4 shows TG curves evidencing that the products obtained by desolvation of the hydrate and solvate materials decompose on fusion.

Table S3. Amounts of Substance n of Water in 5HNA·nH$_2$O Obtained by TG

T_i/K	T_f/K	m_i/mg	Δm/mg	n
372.5	390.1	3.330704	0.367238	0.96
372.3	390.2	4.744623	0.526373	0.96
370.7	389.3	4.869117	0.541364	0.97
372.3	390.7	4.446754	0.495290	0.97
370.4	388.2	3.856289	0.413084	0.93
375.6	394.2	5.510496	0.614892	0.97
374.8	392.2	4.964419	0.539943	0.94
363.4	380.4	6.477902	0.722817	0.97
364.5	381.4	6.166906	0.678637	0.95
365.4	378.3	6.446660	0.707354	0.95
372.5	390.1	3.330704	0.367238	0.96
372.3	390.2	4.744623	0.526373	0.96

$\langle T_i \rangle = 370.2 \pm 2.7$ K; $\langle T_f \rangle = 387.5 \pm 3.4$ K
$\langle n \rangle = 0.96 \pm 0.01$

Table S4. Amounts of Substance n of DMSO in 5HNA·nDMSO Obtained by TG

T_i/K	T_f/K	m_i/mg	Δm/mg	n
390.6	410.9	6.131532	2.238005	1.02
388.8	410.7	5.558332	2.013057	1.01
389.9	409.6	5.853685	2.111103	1.00
387.9	411.6	6.345128	2.290331	1.01
391.2	410.4	6.937745	2.536834	1.03

$\langle T_i \rangle = 389.7 \pm 1.2$ K; $\langle T_f \rangle = 410.6 \pm 0.7$ K
$\langle n \rangle = 1.01 \pm 0.02$

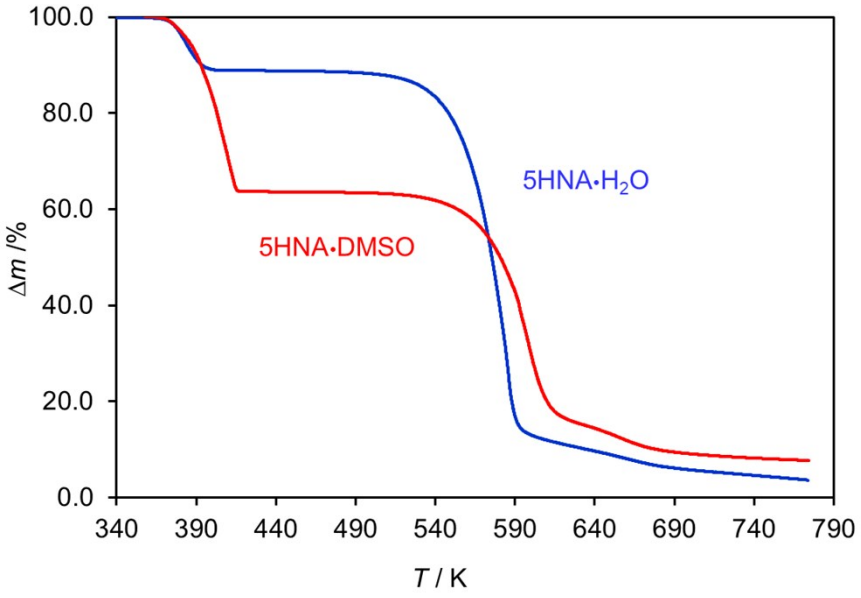

(a)

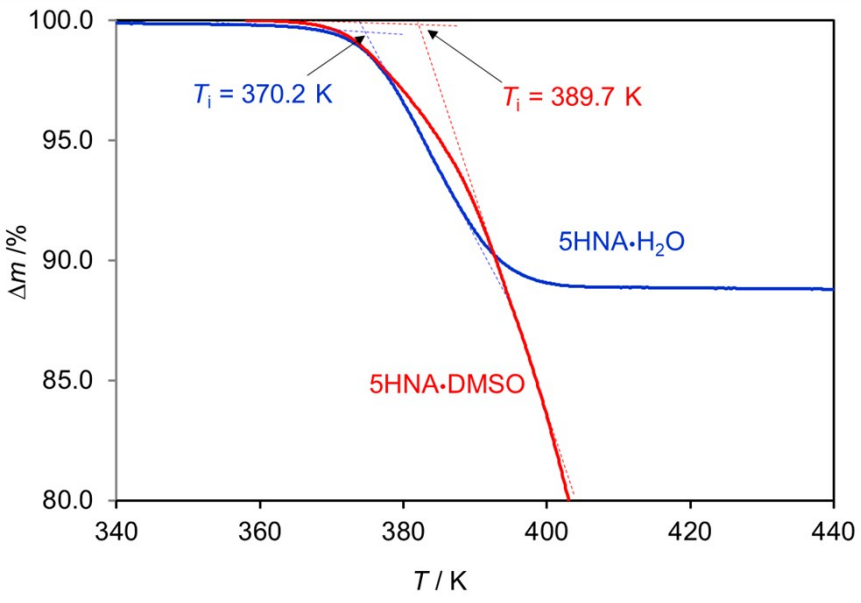

(b)

Figure S4. TG curves obtained at β = 5 K·min^{-1} for 5HNA·H_2O and 5HNA·DMSO showing the mass loss corresponding to thermal decomposition upon fusion: (a) full range; (b) detail of the desolvation onset.

Differential Scanning Calorimetry (DSC). The DSC results obtained for the anhydrous 5HNA at a heating rate of 30 K·min^{-1} are given in Table S5, where: m is the mass of sample; T_{on} and T_{max} are the onset and maximum temperatures of the DSC fusion peak, respectively; and $\Delta_{fus}h_m$ and $\Delta_{fus}H_m$ are the specific and molar enthalpies of fusion.

The study of 5HNA·H_2O and 5HNA·DMSO dehydration/desolvation according to (S = H_2O, DMSO):

$$5HNA\cdot S(cr, T_i) \rightarrow 5HNA(cr, T_f) + S(g, T_f) \qquad (S1)$$

led to the results in Tables S6 and S7, where T_i and T_f are the initial and final temperatures of the dehydration step, respectively, T_{max} is the temperature corresponding to the peak maximum and Δh (eq S1) is the specific enthalpy change.

The uncertainties quoted for $<T_{on}>$, $<T_{max}>$, $<T_i>$, $<T_f>$, $<\Delta_r h\,(\text{eq S1})>$ $\Delta_{fus}h_m$, $<\Delta_{fus}H_m>$, and $<\Delta_r H_m\,(\text{eq S1})$ are twice the standard error of the mean of the number of performed determinations.

Table S5 Results of the DSC Experiments on 5HNA

m/mg	T_{on} /K	T_{max} /K	$\Delta_{fus}h_m$ /(J·g^{-1})
3.362	586.90	594.57	328.89
2.203	589.30	594.87	335.13
2.042	586.20	592.60	335.80
3.239	587.47	593.78	321.95

$<T_{on}>$ = 587.5±1.3 K; $<T_{max}>$ = 594.0±1.0 K

$<\Delta_{fus}h>$ = 330.4±6.5 J·g^{-1}

$M(C_6H_5O_3N)$ = 139.110 g.mol^{-1}

$<\Delta_{fus}H_m>$ = 46.0±0.9 kJ·mol^{-1}

Table S6 Results of the DSC Experiments on 5HNA·H_2O.

m/mg	T_i/K	T_{max}/K	T_f/K	Δh (eq S1)/J·g^{-1}
3.639	368.7	378.9	385.6	362.89
4.295	373.4	379.1	384.7	338.55
4.435	370.9	377.7	382.4	352.49
3.123	368.7	378.8	385.5	353.52
3.140	367.9	378.6	385.4	371.90

$<T_i>$ = 369.9±2.0 K; $<T_{max}>$ = 378.6±0.5 K; $<T_f>$ = 384.7.±1.2 K

$<\Delta_r h$ (eq S1)> = 355.9±11.2 J·g^{-1}

M($C_6H_5O_3N·H_2O$) = 157.125 g.mol^{-1}

$<\Delta_r H_m$ (eq S1)> = 55.9±1.8 kJ·mol^{-1}

Table S7 Results of the DSC Experiments on 5HNA·DMSO.

	First peak			Second peak		
m/mg	T_i/K	T_{max}/K	T_f/K	T_i/K	T_{max}/K	T_f/K
6.330	390.7	396.5	400.4	401.3	449.4	477.6
5.589	387.6	393.1	399.7	413.0	440.3	453.1
5.208	384.9	391.0	397.7	400.3	437.8	450.5
6.407	394.3	399.3	401.9	403.0	443.6	460.8
5.891	389.3	394.5	399.5	400.9	438.1	456.1

First peak: $<T_i>$ = 389.4±3.1 K; $<T_{max}>$ = 394.9±2.8 K; $<T_f>$ = 399.8.±1.4 K

Second peak: $<T_i>$ = 403.7±4.7 K; $<T_{max}>$ = 441.8±4.3 K; $<T_f>$ = 459.6.±9.6 K

M($C_6H_5O_3N·C_2H_6O_2S$) = 217.239 g.mol^{-1}

Calvet microcalorimetry. The Calvet microcalorimetry study of reaction S1 for 5HNA·H_2O and 5HNA·DMSO led to the results in Tables S8 and S9. Here m_s and m_c are the masses of sample and of the glass capillary tube, respectively; A is the area of the measuring curve corresponding to the over-all calorimetric experiment; A_b is the area of the pumping background contribution to the calorimetric process, which was determined in a series separate experiments; ε is the energy equivalent of the calorimeter obtained from a set of electrical calibrations; T_f is the temperature of the calorimetric cell; T_i is the initial temperature of the sample before being dropped into the calorimetric cell; The term $\Delta_r h$ in eq S2 represents the specific enthalpy of the process in eq S1, and was calculated from:

$$\Delta_r h = \frac{1}{m_s}\left[\frac{A - A_b}{\varepsilon} - m_c c_{p,c}(T_f - T_i)\right] \tag{S2}$$

were $\Delta T = T_f - T_i$ and $c_{p,c}$ = 0.787 J·g^{-1} is the average massic heat capacity of the capillary tube at constant pressure in the ΔT range. The value of $c_{p,c}$ was determined in an independent experiment where empty glass capillaries were dropped into the calorimeter. The results in Tables S8 and S9 lead to $\Delta_r h$ = 406.50±3.14 J·g^{-1} for 5HNA·H_2O and $\Delta_r h$ = 461.76±6.47 J·g^{-1} J·g^{-1} for 5HNA·DMSO where the uncertainty quoted represent standard deviations of the mean. These values correspond to $\Delta_r H_m^o$ = 63.9±1.4 kJ·mol^{-1} for 5HNA·H_2O and $\Delta_r H_m^o$ = 100.3±2.8 kJ·mol^{-1} for 5HNA·DMSO, where the assigned uncertainties correspond to twice the over-all standard error of the mean which includes contributions from the main experiment and the calibration.

Table S8. Results of the Calvet Microcalorimetry Experiments on 5HNA·H_2O

m_s/mg	m_c/mg	A/mV·s	T_i/K	T_f/K	Δh (eq S1)/J·g^{-1}
5.320	40.190	262.564	297.983	361.485	403.637
5.318	42.005	270.866	298.032	361.486	411.481
5.918	40.580	276.989	298.035	361.845	396.130
5.918	40.145	279.341	298.236	361.801	407.296
6.838	40.542	307.422	298.238	361.801	413.947

A_b = –2.724 mV·s

ε = 63.833±0.07 mV·W^{-1}

$<T_i>$ = 298.10±0.10 K; $<T_f>$ = 361.68±0.16 K

$<\Delta_r h$ (eq S2)> = 406.50±3.14 J·g^{-1}

$\sigma_{over\text{-}all}$ = 3.18 J·g^{-1}

$M(C_6H_5O_3N\cdot H_2O)$ = 157.125 g.mol^{-1}

$<\Delta_r H_m$ (eq S2)> = 63.9±1.4 kJ·mol^{-1}

Table S9. Results of the Calvet Microcalorimetry Experiments on 5HNA·DMSO.

m_s/mg	m_c/mg	A/mV·s	T_i/K	T_f/K	Δh (eq S1)/J·g^{-1}
8.148	40.577	356.301	297.979	361.361	441.878
9.975	42.018	433.827	297.972	361.377	475.407
9.038	40.594	398.609	298.019	361.392	471.634
8.635	42.012	380.170	297.900	361.476	451.251
9.142	41.543	403.375	297.922	361.472	468.612

A_b = –2.724 mV·s

ε = 63.833±0.07 mV·W^{-1}

$<T_i>$ = 297.96±0.04 K; $<T_f>$ = 361.42±0.05 K

$<\Delta_r h$ (eq S2)> = 461.76±6.47 J·g^{-1}

$\sigma_{over\text{-}all}$ = 6.49 J·g^{-1}

$M(C_6H_5O_3N\cdot C_2H_6OS)$ = 217.239 g.mol^{-1}

$<\Delta_r H_m$ (eq S2)> = 100.3±2.8 kJ·mol^{-1}

Heat capacity data. The values of $\Delta_r H^o_m(\mathrm{A})$, $\Delta_r H^o_m(\mathrm{B})$, and $\Delta_r H^o_m(\mathrm{C})$ in Table 2 of the main text were calculated using equations S3-S5:

$$\Delta_r H^o_m(\mathrm{A}) = \int_{298.15\ \mathrm{K}}^{T_i} C^o_{p,m}(5\mathrm{HNA}\cdot\mathrm{S},\ \mathrm{cr})\mathrm{d}T \tag{S3}$$

$$\Delta_r H^o_m(\mathrm{B}) = \int_{T_f}^{298.15\ \mathrm{K}} C^o_{p,m}(5\mathrm{HNA},\ \mathrm{cr})\mathrm{d}T \tag{S4}$$

$$\Delta_r H^o_m(\mathrm{C}) = \int_{T_f}^{298.15\ \mathrm{K}} C^o_{p,m}(\mathrm{S},\ \mathrm{g})\mathrm{d}T \tag{S5}$$

The integrals in those equations were calculated by using eq S6 ($C^o_{p,m}$ in $\mathrm{J\cdot K^{-1}\cdot mol^{-1}}$ and T in K):

$$C^o_{p,m} = a + bT + cT^2 \tag{S6}$$

and the a, b, and c parameters summarized in Table S10. These were directly taken from the literature or obtained from least squares fittings of eq S6 to reported heat capacity data.[1-4] The heat capacities of 5HNA·H_2O(cr) and 5HNA·DMSO(cr) where estimated as $C^o_{p,m}(5\mathrm{HNA}\cdot\mathrm{S},\ \mathrm{cr}) = C^o_{p,m}(5\mathrm{HNA},\ \mathrm{cr}) + C^o_{p,m}(\mathrm{S},\ \mathrm{cr})$.

Table S10. Coefficients of Eq S6 for Different Compounds in Condensed or Gaseous States

		a	*b*	*c*
5HNA	(cr)[a]	23.501	0.43400	
	(g)[a]	34.367	0.35625	
5HNA·H_2O	(cr)[b]	25.380	0.56583	
5HNA·DMSO	(cr)[b]	49.636	0.74489	
H_2O	(cr)[c]	1.8785	0.13183	
	(g)[c]	33.898	-6.4164×10^{-3}	1.8177×10^{-5}
DMSO	(cr)[d]	117.50	0.11739	
	(g)[d]	24.800	0.25105	-1.1399×10^{-4}

[a] Reference 4. [b] Estimated as $C^{\circ}_{p,\mathrm{m}}(5\mathrm{HNA}\cdot\mathrm{S},\ \mathrm{cr}) = C^{\circ}_{p,\mathrm{m}}(5\mathrm{HNA},\ \mathrm{cr}) + C^{\circ}_{p,\mathrm{m}}(\mathrm{S},\ \mathrm{cr})$. [c] Reference 3. [d] Obtained from least squares fitting of eq S6 to the data for solid DMSO in the range 150-220 K listed in Reference 1 and the data for the gas phase in the range 200-500 K given in Reference 2.

Enthalpy of formation data. The enthalpies of formation of the hydrate, $\Delta_f H^{\circ}_m(5\mathrm{HNA}\cdot\mathrm{H_2O},\ \mathrm{cr}) = -831.5\pm4.8$ kJ·mol^{-1}, and the solvate, $\Delta_f H^{\circ}_m(5\mathrm{HNA}\cdot\mathrm{DMSO}) = -771.8\pm5.7$ kJ·mol^{-1}, could be derived from:

$$\Delta_f H^{\circ}_m(5\mathrm{HNA}\cdot\mathrm{S},\ \mathrm{cr}) = -\Delta_r H^{\circ}_m(2) + \Delta_f H^{\circ}_m(5\mathrm{HNA},\ \mathrm{cr})\ \Delta_f H^{\circ}_m(\mathrm{S},\ \mathrm{g}) + \qquad \text{(S7)}$$

by combining the $\Delta_r H^{\circ}_m(2)$ values in Table 2 of the main text with $\Delta_f H^{\circ}_m(5\mathrm{HNA},\ \mathrm{cr}) = -537.6\pm4.7$ kJ·mol^{-1},[4] $\Delta_f H^{\circ}_m(\mathrm{H_2O},\ \mathrm{g}) = -241.834\pm0.027$ kJ·mol^{-1} [5] and, $\Delta_f H^{\circ}_m(\mathrm{DMSO},\ \mathrm{g}) = -150.5\pm1.5$ kJ·mol^{-1}.[6,7]

Speciation of Aqueous 5-Hydroxynicotinic acid at 295K for Different pH. 5-Hydroxynicotinic acid is an amphiprotic system where four differently charged species may be present in equilibrium (Scheme S1). Their molar fractions $x_{(5HNA)^+}$, $x_{(5HNA)^0}$, $x_{(5HNA)^-}$ and $x_{(5HNA)^{2-}}$ at a given pH, can be approximately predicted from the corresponding acidity constants at 295 K, pK_{a1} = 1.90±0.5, pK_{a2} = 4.66±0.05, pK_{a3} = 8.62±0.04 [8] by using:[9]

$$x_{(5HNA)^+} = \frac{[H^+]^3}{\alpha} \quad \text{(S8)}$$

$$x_{(5HNA)^0} = \frac{K_{a1}[H^+]^2}{\alpha} \quad \text{(S9)}$$

$$x_{(5HNA)^-} = \frac{K_{a1}K_{a2}[H^+]}{\alpha} \quad \text{(S10)}$$

$$x_{(5HNA)^{2-}} = 1 - x_{(5HNA)^+} - x_{(5HNA)^0} - x_{(5HNA)^-} \quad \text{(S11)}$$

$$\alpha = [H^+]^3 + K_{a1}[H^+]^2 + K_{a1}K_{a2}[H^+]^3 + K_{a1}K_{a2}K_{a3} \quad \text{(S12)}$$

The obtained results are shown in Figure S5 and summarized in Table S11, where the data in boldface font correspond to the pH obtained in this work for a saturated 5HNA solution at 295 K.

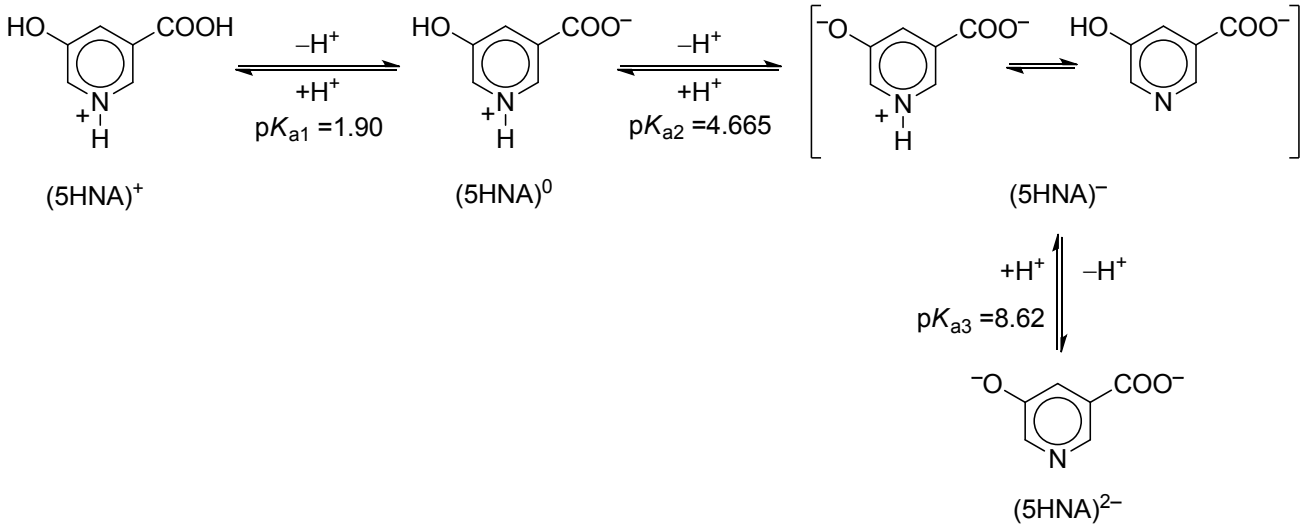

Scheme S1

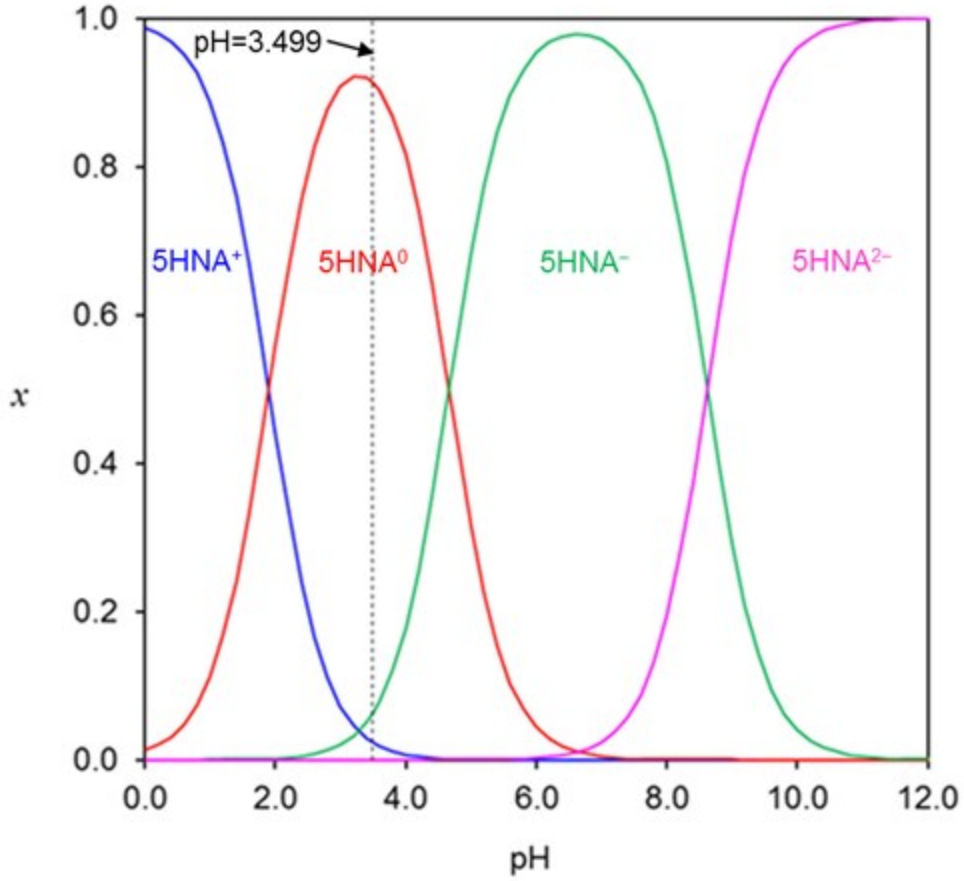

Figure S5. Molar Fractions of the 5-Hydroxynicotinic acid Species Present in Aqueous Solution for Different pHs, at 295 K

Table S11. Molar Fractions of the 5-Hydroxynicotinic Acid Species Present in Aqueous Solution for Different pHs, at 295 K

pH	$x_{(5HNA)^+}$	$x_{(5HNA)^0}$	$x_{(5HNA)^-}$	$x_{(5HNA)^{2-}}$
0.0	0.9876	0.0124	0.0000	0.0000
0.2	0.9804	0.0196	0.0000	0.0000
0.4	0.9693	0.0307	0.0000	0.0000
0.6	0.9523	0.0477	0.0000	0.0000
0.8	0.9264	0.0736	0.0000	0.0000
1.0	0.8882	0.1118	0.0000	0.0000
1.2	0.8336	0.1663	0.0001	0.0000
1.4	0.7596	0.2402	0.0001	0.0001
1.6	0.6659	0.3338	0.0003	0.0000
1.8	0.5570	0.4424	0.0006	0.0000
2.0	0.4421	0.5566	0.0012	0.0001
2.2	0.3331	0.6646	0.0023	0.0000
2.4	0.2393	0.7566	0.0042	-0.0001
2.6	0.1651	0.8277	0.0072	0.0000
2.8	0.1105	0.8774	0.0121	0.0000
3.0	0.0721	0.9080	0.0199	0.0000
3.2	0.0462	0.9218	0.0320	0.0000
3.4	0.0291	0.9203	0.0506	0.0000
3.499	**0.0230**	**0.9139**	**0.0631**	**0.0000**
3.6	0.0180	0.9033	0.0787	0.0000
3.8	0.0109	0.8691	0.1200	0.0000
4.0	0.0065	0.8152	0.1783	0.0000
4.2	0.0037	0.7398	0.2565	0.0000
4.4	0.0020	0.6440	0.3539	0.0001
4.6	0.0011	0.5339	0.4650	0.0000
4.8	0.0005	0.4198	0.5795	0.0002
5.0	0.0002	0.3136	0.6860	0.0002
5.2	0.0001	0.2238	0.7758	0.0003
5.4	0.0000	0.1539	0.8456	0.0005
5.6	0.0000	0.1029	0.8962	0.0009
5.8	0.0000	0.0675	0.9311	0.0014
6.0	0.0000	0.0436	0.9541	0.0023
6.2	0.0000	0.0279	0.9684	0.0037
6.4	0.0000	0.0178	0.9763	0.0059
6.6	0.0000	0.0112	0.9794	0.0094
6.8	0.0000	0.0071	0.9781	0.0148
7.0	0.0000	0.0044	0.9722	0.0234
7.2	0.0000	0.0028	0.9607	0.0365
7.4	0.0000	0.0017	0.9416	0.0567
7.6	0.0000	0.0010	0.9119	0.0871
7.8	0.0000	0.0006	0.8680	0.1314
8.0	0.0000	0.0004	0.8062	0.1934
8.2	0.0000	0.0002	0.7244	0.2754

8.4	0.0000	0.0001	0.6239	0.3760
8.6	0.0000	0.0001	0.5115	0.4884
8.8	0.0000	0.0000	0.3978	0.6022
9.0	0.0000	0.0000	0.2942	0.7058
9.2	0.0000	0.0000	0.2082	0.7918
9.4	0.0000	0.0000	0.1423	0.8577
9.6	0.0000	0.0000	0.0948	0.9052
9.8	0.0000	0.0000	0.0620	0.9380
10.0	0.0000	0.0000	0.0400	0.9600
10.2	0.0000	0.0000	0.0256	0.9744
10.4	0.0000	0.0000	0.0163	0.9837
10.6	0.0000	0.0000	0.0104	0.9896
10.8	0.0000	0.0000	0.0066	0.9934
11.0	0.0000	0.0000	0.0042	0.9958
11.2	0.0000	0.0000	0.0026	0.9974
11.4	0.0000	0.0000	0.0017	0.9983
11.6	0.0000	0.0000	0.0010	0.9990
11.8	0.0000	0.0000	0.0007	0.9993
12.0	0.0000	0.0000	0.0004	0.9996
12.2	0.0000	0.0000	0.0003	0.9997
12.4	0.0000	0.0000	0.0002	0.9998
12.6	0.0000	0.0000	0.0001	0.9999
12.8	0.0000	0.0000	0.0001	0.9999
13.0	0.0000	0.0000	0.0000	1.0000
13.2	0.0000	0.0000	0.0000	1.0000
13.4	0.0000	0.0000	0.0000	1.0000
13.6	0.0000	0.0000	0.0000	1.0000
13.8	0.0000	0.0000	0.0000	1.0000
14.0	0.0000	0.0000	0.0000	1.0000

Computational Chemistry.

Table S12. Electronic Energies (E_{el}), Thermal Corrections (E_v+E_r+E_t), Zero Point Energies (ZPE) and Enthalpies[a] and Gibbs Energies at 298.15 K Obtained for Various 5HNA Conformers by the B3LYP/6-311++G (3df, 3pd) Procedure. Data in Hartree[b]

	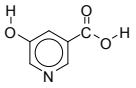	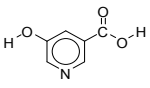	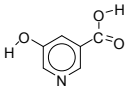	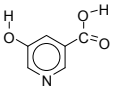	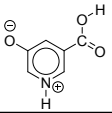	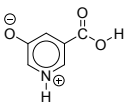	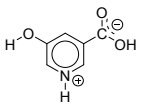	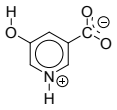
H^o(298.15 K)[a]	-512.181057	-512.180867	-512.180515	-512.180134	-512.159679	-512.158520	-512.136035	-512.131593
G^o(298.15 K)[a]	-512.223738	-512.223595	-512.223287	-512.222907	-512.202366	-512.2012256	-512.178893	-512.174693
ΔH^o(298.15 K)[b]	0	0.5	1.4	2.4	56.1	59.2	118.2	128.8
ΔG^o(298.15 K)[b]	0	0.4	1.2	2.2	56.1	59.0	117.7	129.9

[a] Data in hartree (1 hartree = 2625.5 kJ·mol^{-1}).. [b] Data in kJ·mol^{-1}

References

1. H. L. Clever, E. F. Westrum, Jr., *J. Phys. Chem.*, 1970, **74**, 1309-1317.
2. M. Fulem, K. Růžička, M. Růžička, *Fluid Phase Equilibr.*, 2011, **303**, 205-216.
3. E. P. Matias, C. E. S. Bernardes, M. F. M. Piedade, M. E. Minas da Piedade, *Cryst. Growth Des.*, 2011, **11**, 2803-2810.
4. R. C. Santos, R. M. B. B. M. Figueira, M. F. M. Piedade, H. P. Diogo, M. E. Minas da Piedade, *J. Phys. Chem. B*, 2009, **113**, 14291-14309.
5. B. Ruscic, D. H. Bross, *Active Thermochemical Tables (ATcT) values based on ver. 1.122d of the Thermochemical Network*; available at ATcT.anl.gov, 2015.
6. N. Masuda, Y. Nagano, M. Sakiyama, *J. Chem. Thermodyn.*, 1994, **26**, 971-975.
7. T. B. Douglas, *J. Am. Chem. Soc.*, 1948, **70**, 2001-2002.
8. V. P. Lezina, A. U. Stepanyants, N. I. Golovkina, L. D. Smirnov, *Bull. Acad. Sci. USSR Div. Chem. Sci.*, 1980, **29**, 85-92.
9. P. W. Atkins, J. de Paula, *Physical Chemistry for the Life Sciences*; 5th ed.; Oxford University Press, Oxford, 2006.